IOP FTC
IOP PUBLISHING JOURNAL OF PHYSICS A: MATHEMATICAL AND THEORETICAL

J. Phys. A: Math. Theor. **40** (2007) F771–F784 doi:10.1088/1751-8113/40/31/F03

FAST TRACK COMMUNICATION

Percolation crossing formulae and conformal field theory

Jacob J H Simmons[1], Peter Kleban[1] and Robert M Ziff[2]

[1] LASST and Department of Physics & Astronomy, University of Maine, Orono, ME 04469, USA
[2] Michigan Center for Theoretical Physics and Department of Chemical Engineering, University of Michigan, Ann Arbor, MI 48109-2136, USA

E-mail: Jacob.Simmons@umit.maine.edu, kleban@maine.edu and rziff@umich.edu

Received 5 June 2007
Published 19 July 2007
Online at stacks.iop.org/JPhysA/40/F771

Abstract
Using conformal field theory, we derive several new crossing formulae at the two-dimensional percolation point. High-precision simulation confirms these results. Integrating them gives a unified derivation of Cardy's formula for the horizontal crossing probability $\Pi_{\rm h}(r)$, Watts' formula for the horizontal–vertical crossing probability $\Pi_{\rm hv}(r)$ and Cardy's formula for the expected number of clusters crossing horizontally $\mathcal{N}_{\rm h}(r)$. The main step in our approach implies the identification of the derivative of one primary operator with another. We present operator identities that support this idea and suggest the presence of additional symmetry in $c = 0$ conformal field theories.

PACS numbers: 64.60.Ak, 64.60.Cn, 64.70.−p

(Some figures in this article are in colour only in the electronic version)

1. Introduction

Percolation in two-dimensional systems remains under very active current study, despite a long history. The 2D percolation point has been explored with a wide variety of methods, including conformal field theory (CFT) [1, 2], modular forms [3], computer simulation [2], other field-theoretic methods [4], Stochastic Löwner Evolution (SLE) processes [5] and other rigorous methods [6]. (We cite only a very few representative works since the literature is so extensive.)

Crossing probabilities are of great interest in studies of the percolation point in two dimensions. In geometries with edges, these conformally invariant quantities give the probability that percolation configurations cross between some specified set of intervals on the boundary of the system. Perhaps the best known example is Cardy's equation for the horizontal crossing probability $\Pi_{\rm h}(r)$ [1] (which was later proven rigorously for a particular

realization of percolation [7]). This, the probability that a percolation cluster connects the two vertical sides of a rectangle of aspect ratio (width/length) r, is given by

$$\Pi_{\mathrm{h}}(\lambda) = C\lambda^{1/3}{}_2F_1(1/3, 2/3; 4/3; \lambda), \tag{1}$$

with $C = 2\pi\sqrt{3}/\,\Gamma\left(\frac{1}{3}\right)^3 = 0.566\,046\,68\ldots$. The cross-ratio λ is related to r by conformally mapping three consecutive corners of the rectangle to 1, ∞ and 0 so that the fourth corner lies on the point λ, with $0 \leqslant \lambda \leqslant 1$. The interior of the rectangle maps to the upper half-plane. Cardy used arguments of conformal field theory; primarily that the (boundary) operator which changes free to fixed boundary conditions on an edge of the system is $\psi_1 := \phi_{1,2}$ in the $c = 0$ Kac table (the notation $\psi_n := \phi_{1,n+1}$ simplifies the expressions for the boundary operator product expansion coefficients considered below [8]).

The probability $\Pi_{\mathrm{hv}}(r)$ that all four sides of the rectangle are connected by a single percolating cluster was determined by Watts [9], using an extension of Cardy's arguments (see also the recent rigorous proof of Dubédat [5]). This may be written as

$$\Pi_{\mathrm{hv}}(\lambda) = \Pi_{\mathrm{h}}(\lambda) - \Pi_{\mathrm{h\bar{v}}}(\lambda), \tag{2}$$

where $\Pi_{\mathrm{h\bar{v}}}$ denotes the probability of a horizontal crossing without a vertical crossing,

$$\Pi_{\mathrm{h\bar{v}}}(\lambda) = \frac{\sqrt{3}}{2\pi}\lambda_3F_2(1, 1, 4/3; 5/3, 2; \lambda). \tag{3}$$

To derive this result, Watts made use of a higher-order null vector in the $c = 0 = h$ Verma module.

Finally, the expected number of clusters crossing horizontally, $\mathcal{N}_{\mathrm{h}}(r)$, has also been determined by Cardy [10, 11] (and later via rigorous methods [12]). This calculation involves identifying percolation as the $q \to 1$ limit of the q-state Potts model and taking a derivative with respect to q at $q = 1$. Maier [13] pointed out that the result may be expressed as

$$\mathcal{N}_{\mathrm{h}}(\lambda) = \Pi_{\mathrm{h}}(\lambda) - \frac{1}{2}\Pi_{\mathrm{h\bar{v}}}(\lambda) + \frac{\sqrt{3}}{4\pi}\ln\left(\frac{1}{1-\lambda}\right). \tag{4}$$

The motivation for this paper is the remark by Maier [13] that the fifth-order differential equation which arises from the null vector used by Watts [9] to determine Π_{hv} has, among its additional solutions [3], both Π_{h} and $\mathcal{N}_{\mathrm{h}}$. This mathematical observation has, to our knowledge, eluded explanation. In this paper, using a simple adaptation of Cardy's method, we give a unified derivation of all three formulae. In section 2 we calculate Π_{h}, based on a physical interpretation of the $\psi_3 := \phi_{1,4}$ operator. Section 3 extends this method to three new crossing formulae. Numerical verification of these results is given in section 4; by integrating them, the three known crossing quantities are reproduced in section 5. Our derivation makes use of primary operators only, avoiding higher-order null vectors and does not require reference to the Potts models to obtain $\mathcal{N}_{\mathrm{h}}$. Then, in section 6, we point out that our method implies proportionality of ψ_3 and the derivative of ψ_1, and explore some further consequences of this identification.

2. Cardy's equation revisited

In this section, we briefly review Cardy's derivation of the horizontal crossing probability $\Pi_{\mathrm{h}}(\lambda)$, and then present the approach used to derive it here, as an introduction to the more interesting results below.

In [1] Cardy determined $\Pi_{\mathrm{h}}(\lambda)$ via the four-point function $\langle\psi_1(0)\psi_1(\lambda)\psi_1(1)\psi_1(\infty)\rangle$. Here, adjacent pairs of operators mark the intervals $(0, \lambda)$ and $(1, \infty)$ between which the crossing occurs.

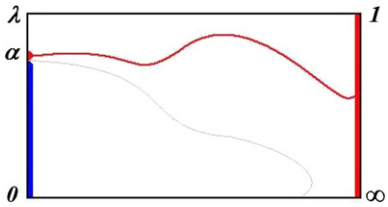

Figure 1. Effects of $\psi_3(\alpha)$-configurations contributing to $\Pi_{\mathrm{h};\alpha}$. Crossing path shown in red, dual path in grey. Thick (thin) boundary lines represent fixed (free) edges.

Our figures herein are shown as rectangles, while our formulae are given in terms of upper half-plane variables, e.g., λ. These two geometries are equivalent under a conformal mapping. One visualizes crossings in rectangles for consistency with common usage (e.g. 'horizontal crossing'), but takes parameters to lie on the real line for mathematical simplicity. Thus 'the $(0, \lambda)$ edge of the rectangle' in fact indicates the interval on the real axis that maps into the corresponding side of the rectangle. Figure 1 illustrates how the four points $(0, \lambda, 1, \infty)$ on the real axis map to the rectangle.

Cardy's derivation (see [1] or [10] for more details) focuses on the comparison of the two possible fixed boundary condition assignments: either the same or different. For percolation, a fixed boundary either allows clusters to touch it or not; thus a rectangle with two fixed vertical edges and free horizontal edges either includes all clusters or excludes horizontally crossing clusters. Therefore, by inserting a ψ_1 (which changes the boundary condition from fixed to free) at each of the four corners of the rectangle, and considering the second-order differential equation implied by their null vector, one finds two solutions, which may be taken to be 1 and $\Pi_{\mathrm{h}}(\lambda)$. Thus,

$$\Pi_{\mathrm{h}}(\lambda) = \left\langle \psi_1^{af}(0)\psi_1^{fa}(\lambda)\psi_1^{af}(1)\psi_1^{fa}(\infty)\right\rangle - \left\langle \psi_1^{af}(0)\psi_1^{fb}(\lambda)\psi_1^{bf}(1)\psi_1^{fa}(\infty)\right\rangle. \tag{5}$$

Here, the superscripts indicate the boundary condition change; f denoting free and a or b fixed boundary conditions, with $a \neq b$. Thus, the first term includes all configurations, and is a constant, independent of λ, while the second removes those configurations with no horizontal crossing. If we normalize our (boundary) operators so that $\langle \psi_i(0)\psi_i(x)\rangle = x^{-2h_i}$, it follows that the two sides of (5) are equal, with no multiplicative constant, and (5) becomes

$$\Pi_{\mathrm{h}}(\lambda) = 1 - \Pi_{\mathrm{h}}(1-\lambda), \tag{6}$$

which may also be derived using duality (see [1, 10] for more details on these matters).

Our method modifies the standard derivation as follows. Consider the probability density $\Pi_{\mathrm{h};\alpha}$ that the crossing connects the interval $(\alpha, \alpha + \mathrm{d}\alpha)$ but *not* the interval $(0, \alpha)$ to the interval $(1, \infty)$, where $0 \leqslant \alpha \leqslant \lambda \leqslant 1$. This is

$$\Pi_{\mathrm{h};\alpha}\,\mathrm{d}\alpha = \Pi_{\mathrm{h}}(\alpha + \mathrm{d}\alpha) - \Pi_{\mathrm{h}}(\alpha) \quad \Rightarrow \quad \Pi_{\mathrm{h};\alpha} = \partial_\alpha \Pi_{\mathrm{h}}(\alpha). \tag{7}$$

The configurations that will contribute to this probability are those which have a percolation cluster connecting the point α to the interval $(1, \infty)$ and also have, on the fixed boundary side of that percolation cluster, a dual path from α to $(-\infty, 0)$, as illustrated in figure 1. Here, the fact that the small interval is not connected to $(0, \alpha)$ ensures the presence of the dual path; and the differentiation in (7) removes the constant term in (5), so that a crossing cluster must attach to α.

At first sight, it might seem that $\Pi_{\mathrm{h};\alpha}$ should also depend on λ. However, this quantity, which is specified in the half-plane, can be mapped to a rectangle with any aspect ratio r, as mentioned. When this is done, the length of the image of the interval $(0, \alpha)$ will vary according to λ, which also determines r.

Now the operator expected [6, 8] to generate a percolation cluster and dual path should have dimension $h = 1$. This suggests that it is $\psi_3 := \phi_{1,4}$. For the moment we simply assume this and explore its consequences. In section 6, we give a better justification (and consider its implications).

Note that ψ_3, since it arises in the operator product expansion of three ψ_1 operators, must sit at a fixed-free boundary change, as shown in figure 1.

Therefore, we have

$$\Pi_{\mathrm{h};\alpha} = K\langle\psi_1(0)\psi_3(\alpha)\psi_1(1)\psi_1(\infty)\rangle, \tag{8}$$

where K is a constant. If we set

$$K = \frac{3^{1/4}}{2\sqrt{\pi}}, \tag{9}$$

it turns out that (8) will be properly normalized, as shown below. In section 6, we justify (9) directly, without reference to percolation, by means of the operator product expansion. Note that K^2 is exactly $1/2$ the constant appearing in (3).

Thus,

$$\begin{aligned}\Pi_{\mathrm{h}}(\lambda) &= \int_0^\lambda \Pi_{\mathrm{h};\alpha}\,\mathrm{d}\alpha \\ &= K\int_0^\lambda \left\langle\psi_1^{fa}(0)\psi_3^{af}(\alpha)\psi_1^{fb}(1)\psi_1^{bf}(\infty)\right\rangle \mathrm{d}\alpha.\end{aligned} \tag{10}$$

Therefore, we must determine the correlation function (8). Now we may write

$$\langle\psi_1(x_4)\psi_1(x_3)\psi_3(x_2)\psi_1(x_1)\rangle = \frac{(x_4-x_1)(x_4-x_3)}{(x_3-x_1)(x_4-x_2)^2}F\left(\frac{(x_2-x_1)(x_4-x_3)}{(x_3-x_1)(x_4-x_2)}\right). \tag{11}$$

Since ψ_1 is, as mentioned, a level-two operator, the space of possible solutions for (11) is two dimensional. However, in the operator product expansions of $\psi_1\psi_1$ and $\psi_1\psi_3$, the only common term is $\psi_2 := \phi_{1,3}$, so only one conformal block enters, i.e. the solution space is one dimensional. To determine it, we apply the null state condition to two different ψ_1 operators in (11). This gives two different second-order differential equations for F. Subtracting them so as to cancel the highest-order term gives

$$0 = F'(\alpha) + \frac{2(1-2\alpha)}{3\alpha(1-\alpha)}F(\alpha). \tag{12}$$

This equation fixes the single conformal block as

$$\mathcal{F}^2_{13,11}(\alpha) = (\alpha(1-\alpha))^{-2/3}, \tag{13}$$

where the superscript 2 refers to $\psi_2 := \phi_{1,3}$ which appears in the operator product expansion of ψ_1, both with itself and with ψ_3. (Our conformal blocks are normalized so that $\mathcal{F}^n_{ij,kl}(x) \sim x^{h_n-h_i-h_j}$.) This leads to

$$\left\langle\psi_1^{fa}(0)\psi_3^{af}(\alpha)\psi_1^{fb}(1)\psi_1^{bf}(\infty)\right\rangle = C_{123}C_{112}(\alpha(1-\alpha))^{-2/3}, \tag{14}$$

where the usual superscripts (indicating the boundary conditions) on the boundary operator product expansion coefficients C_{ijk} [14] have been suppressed, as a consequence of duality [8]. Inserting this correlation function into (10) then reproduces (1)

$$\begin{aligned}\Pi_{\mathrm{h}}(\lambda) &= KC_{123}C_{112}\int_0^\lambda \alpha^{-2/3}(1-\alpha)^{-2/3}\,\mathrm{d}\alpha \\ &= 3KC_{123}C_{112}\lambda^{1/3}{}_2F_1(1/3, 2/3; 4/3; \lambda) \\ &= C\lambda^{1/3}{}_2F_1(1/3, 2/3; 4/3; \lambda),\end{aligned} \tag{15}$$

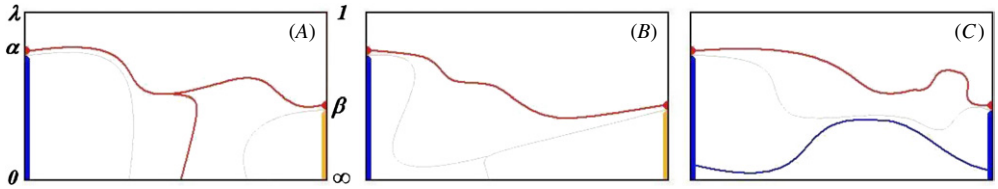

Figure 2. Configurations consistent with $\langle\psi_1(\infty)\psi_3(\beta)\psi_3(\alpha)\psi_1(0)\rangle$.

where we have made use of (9) as well as $C_{123} = 2\sqrt{2\pi}/3\Gamma[1/3]^{3/2}$ and $C_{112} = \sqrt{2\pi}3^{1/4}/\Gamma[1/3]^{3/2}$ [8].

The function $\pi_{\mathrm{h};\alpha} := \partial_\alpha \Pi_{\mathrm{h}}(\alpha)$ is a simple example of what we call a *first-crossing density*. The term 'first' indicates a probability density for configurations that, when we start at the origin and move towards the point λ, first contain a crossing cluster in the neighbourhood of α. Herein, the lower case (π) distinguishes crossing probability *densities* from crossing *probabilities*, represented with upper case (Π).

With only one ψ_3 in the correlation function we reproduce Cardy's result for $\Pi_{\mathrm{h}}(\lambda)$. However by inserting an additional ψ_3 operator we can generate more complicated first (and other) crossing densities. These then give a new derivation of Watts' equation for Π_{hv} [9], and Cardy's expression for the mean number of horizontal crossing clusters $\mathcal{N}_{\mathrm{h}}(\lambda)$ [10, 11], as well as Π_{h}.

3. New crossing formulae

In order to find new results, we consider the correlation function $\langle\psi_1(\infty)\psi_3(\beta)\psi_3(\alpha)\psi_1(0)\rangle$ with $0 < \alpha < \lambda$, and $1 < \beta$. By a simple extension of the argument above, one sees that there are three configurations consistent with this function, illustrated in figure 2.

Let $\pi_{\mathrm{h}}^{b}(\alpha, \beta)$ $\left(\pi_{\mathrm{h}}^{\bar{b}}(\alpha, \beta)\right)$ denote the first-crossing probability density for configurations of type A (B); first crossings from α to β that also make (do not make) contact with the bottom edge of the rectangle.

Similarly, $\nu_{\mathrm{h}}(\alpha, \beta)$ denotes the crossing density of configurations of type C. Now $\nu_{\mathrm{h}}(\alpha, \beta)$ is not a *first* crossing density; rather it includes configurations with crossings from α to β that are not the first crossing, but are distinct from previous crossings—hence the notation ν in place of π. Thus configurations with multiple crossings contribute to $\nu_{\mathrm{h}}(\alpha, \beta)$ for each pair of values α and β spanned by a new cluster. Integrating it therefore counts configurations with n horizontal crossings $n - 1$ times. We use this below to calculate $\mathcal{N}_{\mathrm{h}}(\lambda)$.

Now the correlation function

$$\langle\psi_1(x_4)\psi_3(x_3)\psi_3(x_2)\psi_1(x_1)\rangle = \left(\frac{x_4 - x_1}{(x_4 - x_2)(x_3 - x_1)}\right)^2 F\left(\frac{(x_2 - x_1)(x_4 - x_3)}{(x_3 - x_1)(x_4 - x_2)}\right). \tag{16}$$

It follows that

$$\langle\psi_1(\infty)\psi_3(\beta)\psi_3(\alpha)\psi_1(0)\rangle = \beta^{-2}F(\alpha/\beta). \tag{17}$$

Utilizing the second-order null vector for ψ_1 we find

$$0 = F''(x) + \frac{2(1 - 8x)}{3x(1 - x)}F'(x) - \frac{2(1 - 6x^2)}{3x^2(1 - x)^2}F(x). \tag{18}$$

Solving and selecting the appropriate conformal blocks gives

$$\mathcal{F}^{2}_{13,31}(x) = \frac{1+x}{(1-x)^{5/3}x^{2/3}} \tag{19}$$

$$\mathcal{F}^{4}_{13,31}(x) = \frac{5(1+2x-(1-x^2)_2F_1(1,4/3,5/3,x))}{6(1-x)^2} \tag{20}$$

$$\mathcal{F}^{0}_{33,11}(1-x) = \frac{(1+2x+(1-x^2)_2F_1(1,4/3,5/3,1-x))}{3(1-x)^2} \tag{21}$$

$$\mathcal{F}^{2}_{33,11}(1-x) = \frac{1+x}{2(1-x)^{5/3}x^{2/3}}, \tag{22}$$

with superscripts defined as in (13). The crossing symmetry relations for these conformal blocks follow using hypergeometric identities [15] for $x \to 1-x$, and may be written using the operator product expansion coefficients C_{123} and C_{112} quoted above; we also make use of $C_{233} = 2^{7/2}\pi^{3/2}/3^{9/4}\Gamma[1/3]^{3/2}$ and $C_{134} = \sqrt{2/5}$ [8] (note that $K = C_{112}/3C_{123}$, see (9)). (We have explicitly verified that the hypergeometric identities are consistent with these values.) Thus,

$$C^2_{123}\mathcal{F}^{2}_{13,31}(x) = C_{112}C_{233}\mathcal{F}^{2}_{33,11}(1-x) \tag{23}$$

$$C^2_{134}\mathcal{F}^{4}_{13,31}(x) = \mathcal{F}^{0}_{33,11}(1-x) - C_{112}C_{233}\mathcal{F}^{2}_{33,11}(1-x) \tag{24}$$

$$\mathcal{F}^{0}_{33,11}(1-x) = C^2_{123}\mathcal{F}^{2}_{13,31}(x) + C^2_{134}\mathcal{F}^{4}_{13,31}(x). \tag{25}$$

Given these blocks, we may use the boundary conditions to determine which configurations they correspond to. Fixing both intervals $(0,\alpha)$ and (β,∞) in the same way determines the conformal block, so that

$$\left\langle \psi_1^{fa}(\infty)\psi_3^{af}(\beta)\psi_3^{fa}(\alpha)\psi_1^{af}(0)\right\rangle = \beta^{-2}\mathcal{F}^{0}_{33,11}(1-\alpha/\beta). \tag{26}$$

With the same boundary condition on these two intervals none of the configurations in figure 2 are excluded. Thus (26) is proportional to the sum of all three crossing densities.

Multiplying by K^2 (see (9)) again results in proper normalization, as explained below. Hence,

$$\pi^{b}_{\mathrm{h}}(\alpha,\beta) + \pi^{\bar{b}}_{\mathrm{h}}(\alpha,\beta) + \nu_{\mathrm{h}}(\alpha,\beta) = K^2\beta^{-2}\mathcal{F}^{0}_{33,11}(1-\alpha/\beta). \tag{27}$$

On the other hand, fixing the two intervals $(0,\alpha)$ and (β,∞) differently leads to

$$\left\langle \psi_1^{fb}(\infty)\psi_3^{bf}(\beta)\psi_3^{fa}(\alpha)\psi_1^{af}(0)\right\rangle = C_{112}C_{233}\beta^{-2}\mathcal{F}^{2}_{33,11}(1-\alpha/\beta). \tag{28}$$

In this case configurations of type C are excluded so that

$$\pi^{b}_{\mathrm{h}}(\alpha,\beta) + \pi^{\bar{b}}_{\mathrm{h}}(\alpha,\beta) = K^2C_{112}C_{233}\beta^{-2}\mathcal{F}^{2}_{33,11}(1-\alpha/\beta). \tag{29}$$

Using (24), (27) and (29) we can now find the crossing density

$$\nu_{\mathrm{h}}(\alpha,\beta) = K^2\beta^{-2}\left(\mathcal{F}^{0}_{33,11}(1-\alpha/\beta) - C_{112}C_{233}\mathcal{F}^{2}_{33,11}(1-\alpha/\beta)\right) \tag{30}$$

$$= K^2C^2_{134}\beta^{-2}\mathcal{F}^{4}_{13,31}(\alpha/\beta). \tag{31}$$

To separate $\pi^{b}_{\mathrm{h}}(\alpha,\beta)$ and $\pi^{\bar{b}}_{\mathrm{h}}(\alpha,\beta)$ we fix the boundary conditions on the bottom edge $(-\infty,0)$ to differentiate first crossings that touch the bottom edge (type A) and those that do not (type B or C).

The two-point function

$$\left\langle \psi_3^{af}(\alpha)\psi_3^{fa}(\beta)\right\rangle = (\beta-\alpha)^{-2} \tag{32}$$

includes clusters connecting α and β, but not touching the bottom edge, since it is part of a single fixed interval isolated by a dual path. This excludes crossings of type A, so that

$$\pi_{\rm h}^{\bar{b}}(\alpha,\beta)+\nu_{\rm h}(\alpha,\beta)=K^2(\beta-\alpha)^{-2}. \tag{33}$$

This leads to

$$\pi_{\rm h}^{b}(\alpha,\beta)=K^2\big(\beta^{-2}\mathcal{F}^0_{33,11}(1-\alpha/\beta)-(\beta-\alpha)^{-2}\big) \tag{34}$$

$$\pi_{\rm h}^{\bar{b}}(\alpha,\beta)=K^2\big((\beta-\alpha)^{-2}-C^2_{134}\beta^{-2}\mathcal{F}^4_{13,31}(\alpha/\beta)\big). \tag{35}$$

Collecting and simplifying these results gives the formulae

$$\pi_{\rm h}^{b}(\alpha,\beta)=\frac{(\beta+\alpha)_2F_1(1,4/3,5/3,1-\alpha/\beta)-2\beta}{4\pi\sqrt{3}\beta^2(\beta-\alpha)} \tag{36}$$

$$\pi_{\rm h}^{\bar{b}}(\alpha,\beta)=\frac{(\beta+\alpha)_2F_1(1,4/3,5/3,\alpha/\beta)+2\beta}{4\pi\sqrt{3}\beta^2(\beta-\alpha)} \tag{37}$$

$$\nu_{\rm h}(\alpha,\beta)=\frac{\beta^2+2\alpha\beta-(\beta^2-\alpha^2)_2F_1(1,4/3,5/3,\alpha/\beta)}{4\pi\sqrt{3}\beta^2(\beta-\alpha)^2}. \tag{38}$$

These results are new, to our knowledge. They are sufficient to reproduce all three previously known crossing quantities, as we now proceed to demonstrate. It is interesting that only a single $({}_2F_1)$ hypergeometric function enters.

4. Numerical verification

To verify these results, we carried out simulations using hull walks on a square system, for bond percolation on the square lattice, where $p_c = 1/2$. For this system, a hull walk is a simple walk at 45° to the bonds that turns left or right with equal probability at each step, except when it encounters a site previously visited, in which case it always turns to avoid retracing its path. In this way, the walk lays down the adjacent occupied and vacant bonds of a hull for the percolating system [16, 17]. We tested the functions $\pi_{\rm h}^{b}(\alpha,\beta)$, $\pi_{\rm h}^{\bar{b}}(\alpha,\beta)$ and $\nu_{\rm h}(\alpha,\beta)$ for the half-plane transformed to a square system of side length 1, with α chosen to correspond to $(x, y) = (0, 1/2)$ (the mid-point on the left-hand boundary), and $1 \leqslant \beta \leqslant \infty$, so the corresponding point varies along the right-hand boundary.

In the simulation, the walk was started on the left-hand side of the square at the point $(0, 1/2)$. The requirement that the hull borders a first-crossing cluster starting at that point means that the hull cannot touch anywhere on the entire left-hand side. Similarly, if the hull crosses the top boundary, then the trial is terminated, since that event corresponds to the vacant bonds of the hull touching the top, preventing a horizontal crossing. Walks that touch the lower boundary (indicating the cluster of occupied bonds touches that boundary) were allowed to continue. Those walks that touch the bottom and continue to the cross to the right-hand side contribute to $\pi_{\rm h}^{b}$; those crossing ones that do not touch the bottom were further checked for crossing clusters below them. To do this, a second hull walk was started from $(0, 1/2)$, to represent the hull of the dual crossing, as in the shaded dual-lattice paths shown in figure 5. If this walk intersects the bottom, there cannot be any horizontal crossing clusters below the first simulated crossing cluster, and the walk contributes to $\pi_{\rm h}^{\bar{b}}$. Otherwise, if it does not touch the bottom before it crosses, there must be at least one lower horizontal crossing and the event contributes to $\nu_{\rm h}$.

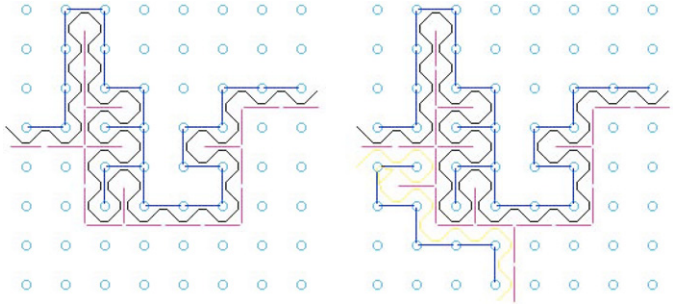

Figure 3. Hull-generating walk algorithm to check for crossing densities on an 8×8 lattice. (Left) a hull (solid curved line) corresponding to a crossing cluster that does not touch left or bottom boundaries and does not cross the top boundary. (Right) second hull walk (shown below the first) showing that there are no lower crossing clusters. (Left) Upper solid straight line segments: occupied bonds on the lattice. Lower segments: bonds on the dual lattice, corresponding to vacant bonds on the original lattice. (Right) An additional set of occupied bonds on the lattice on the lower left, bounding the second hull walk.

Figure 3 shows an example of a walk on a system of 8×8 bonds. Here, the blue circles are lattice vertices and the blue edges occupied bonds on the lattice. The red edges are occupied bonds on the dual lattice, corresponding to vacant bonds on the original lattice. The figure on the left shows, in black, the walk corresponding to a crossing cluster. The system is prepared by setting one vacant bond (or a dual-lattice bond, red) immediately below the lattice point corresponding to $(0, 1/2)$, so that the walk is guaranteed to enter the system and the point $y = 1/2$ will be at the boundary between occupied and vacant bonds. (Walks that exit the system at the entry point are discarded.) The walk then generates the remaining occupied and vacant bonds of the hull. This particular walk terminated when it intersected the right boundary. Next, to check if it was a *first-crossing* cluster, a second hull was initiated, starting on the vacant (or dual-lattice) bond in the first column. This hull is shown in yellow, in the figure on the right. To keep the second walk from leaving the system on the left, we added occupied bonds in the lower first column. This particular walk reached the bottom before reaching the right-hand side, indicating that there were no additional crossing clusters below the first-crossing cluster.

Because this method generates only the hull of the cluster, and simultaneously yields the type of crossing, it is very efficient. In several days of computer time, we were able to generate 3.3×10^{11} hulls on a lattice of 512×512 bonds. Only 0.001 6505 of the walks succeeded in making it across without hitting the top or left-hand sides. Of these, a fraction 0.6456 hit the bottom and contributed to π_{h}^{b}, while the remaining 0.3544 crossed without hitting the bottom. Of the latter, a fraction 0.929 82 did not have additional clusters below them (contributing to $\pi_{\mathrm{h}}^{\bar{b}}$) and 0.070 18 did (contributing to ν_{h}). In all, only a fraction 0.000 1707 of all initiated walks corresponded to events that contribute to ν_{h}.

The above fraction of multiple crossing events, 0.070 18, is somewhat above the predicted value 0.069 189, which is found by integrating the formulae for ν_{h} and $\pi_{\mathrm{h}}^{\bar{b}}$ and taking the ratio of the integral of the former to the sum of the integrals of the former and latter. This difference can be attributed to finite-size effects, which is apparent by considering this quantity for lattices of side length $L = 64(0.076\,53), 128(0.072\,94), 256(0.071\,08)$, and $1024(0.069\,78)$. The data fit very well to a straight line when plotted as a function of $1/L$, with an intercept of 0.069 28, quite close to the predicted value.

In figure 4, we compare the numerical results with the theory. The data are plotted versus the position of the point on the right-hand side corresponding to β, where on the left-hand

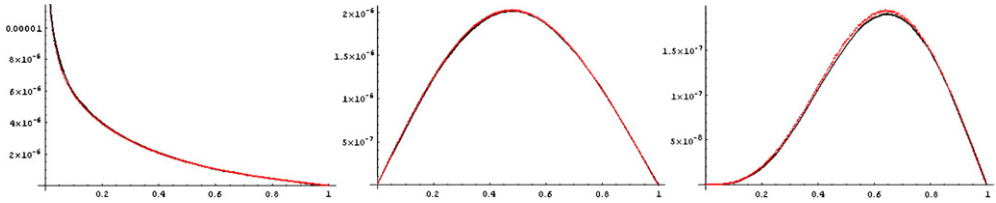

Figure 4. Comparison of simulation (dots) on a 512×512 lattice with theory (equations (36), (37) and (38)).

side we pick the mid-point, as mentioned above. The continuum coordinate was taken to be $y = (Y + 1/2)/512$, where the lattice coordinate $Y = 0, 1, \ldots, 511$. The relative difference between the two curves is on the order of 2%, except near the corners of the square and where the functions are small, in which case the difference is somewhat larger. The overall deviation in ν_h compared with the theory is also a finite-size effect which extrapolates nearly to zero when $L \to \infty$. There is also a slight bias to our results reflecting the fact that a finite system is not perfectly symmetric with respect to the boundary conditions of the walk entering and leaving the system. We have found that this bias also diminishes as the system size increases.

In conclusion, we find very good agreement between simulations and theory for these various quantities.

5. Unified derivation of crossing formulae

Next we integrate our formulae, to re-derive the known results for the horizontal crossing probability Π_h, the horizontal–vertical crossing probability Π_{hv} and the expected number of horizontal crossing clusters $\mathcal{N}_h(\lambda)$.

Now $\Pi_h^b(\lambda)$, the probability that there exists a horizontal crossing cluster that also touches the bottom edge of the rectangle (such as the one illustrated in figure 2(*A*)), is given by

$$\begin{aligned}\Pi_h^b(\lambda) &= \int_0^\lambda \int_1^\infty \pi_h^b(\alpha, \beta)\, \mathrm{d}\beta\, \mathrm{d}\alpha \\ &= \int_0^\lambda \int_1^\infty \frac{(\beta+\alpha)_2F_1(1, 4/3, 5/3, 1-\alpha/\beta) - 2\beta}{4\pi\sqrt{3}\beta^2(\beta-\alpha)}\, \mathrm{d}\beta\, \mathrm{d}\alpha. \end{aligned} \tag{39}$$

(Note that there can only be one such cluster in any configuration, so $\Pi_h^b(\lambda)$ is also the expected number of this type of cluster.) Next let $\beta \to \alpha/\xi$, so that

$$\Pi_h^b(\lambda) = \int_0^\lambda \frac{1}{4\pi\sqrt{3}\alpha} \int_0^\alpha \frac{(1+\xi)_2F_1(1, 4/3, 5/3, 1-\xi) - 2}{(1-\xi)}\, \mathrm{d}\xi\, \mathrm{d}\alpha, \tag{40}$$

then transform the hypergeometric function with the same identities used in deriving the crossing symmetries (23)–(25). This gives

$$\begin{aligned}\Pi_h^b(\lambda) = &\int_0^\lambda \frac{C_{112}^2}{9\alpha} \int_0^\alpha \frac{1+\xi}{(1-\xi)^{5/3}\xi^{2/3}}\, \mathrm{d}\xi\, \mathrm{d}\alpha \\ &- \int_0^\lambda \frac{1}{4\pi\sqrt{3}\alpha} \int_0^\alpha \frac{(1+\xi)_2F_1(1, 4/3, 5/3, \xi) + 2}{(1-\xi)}\, \mathrm{d}\xi\, \mathrm{d}\alpha. \end{aligned} \tag{41}$$

(The coefficient of the first integral is given in terms of C_{112}^2 for reasons that will be clear shortly.) The identity

$$\partial_\xi(3\xi\, {}_2F_1(1, 4/3, 5/3, \xi)) = \frac{(1+\xi)_2F_1(1, 4/3, 5/3, \xi) + 2}{(1-\xi)} \tag{42}$$

follows from the integral representation of the hypergeometric function. Using it in (41) leads to

$$\Pi_{\rm h}^{b}(\lambda) = \int_0^{\lambda} \frac{C_{112}^2}{3\alpha^{2/3}(1-\alpha)^{2/3}}\,{\rm d}\alpha - \frac{\sqrt{3}}{4\pi}\int_0^{\lambda} {}_2F_1(1, 4/3, 5/3, \alpha)\,{\rm d}\alpha. \tag{43}$$

By (15), the first term equals $\Pi_{\rm h}(\lambda)$. To evaluate the second integral we use the identity

$$\partial_\alpha(\alpha\, {}_3F_2(1, 1, 4/3; 5/3, 2; \alpha)) = {}_2F_1(1, 4/3, 5/3, \alpha), \tag{44}$$

which is easily derived from the series for the hypergeometric function. The final result is

$$\begin{aligned}\Pi_{\rm h}^{b}(\lambda) &= \Pi_{\rm h}(\lambda) - \frac{\sqrt{3}}{4\pi}\lambda\, {}_3F_2(1, 1, 4/3; 5/3, 2; \lambda)\\ &= \Pi_{\rm h}(\lambda) - \frac{1}{2}\Pi_{\rm h\bar{v}}(\lambda),\end{aligned} \tag{45}$$

where we have made use of (3).

The treatment for $\Pi_{\rm h}^{\bar{b}}(\lambda)$, the probability of horizontal crossing when the lowest spanning cluster does *not* touch the bottom, follows analogously. Integrating $\pi_{\rm h}^{\bar{b}}(\alpha, \beta)$ over α and β as above, we arrive at the second term in (41). Thus

$$\Pi_{\rm h}^{\bar{b}}(\lambda) = \tfrac{1}{2}\Pi_{\rm h\bar{v}}(\lambda). \tag{46}$$

Equations (45) and (46) allow us to derive $\Pi_{\rm hv}(\lambda)$. The configurations that contribute to $\Pi_{\rm h}^{\bar{b}}(\lambda)$ (figure 2(B)) are such that the crossing from α to β is the first *and* does not touch the bottom edge. Thus the dual path from α to β must itself touch the bottom edge. Therefore, by duality, $\pi_{\rm h}^{\bar{b}}(\alpha, \beta)$ is the probability density of a horizontal crossing that touches the bottom but is separated from the top by a dual cluster from α to β. Thus $\Pi_{\rm h}^{\bar{b}}(\lambda) = \Pi_{\rm h\bar{v}}^{b}(\lambda)$, where $\Pi_{\rm h\bar{v}}^{b}(\lambda)$ is the probability of a horizontal crossing cluster that touches the bottom, but is prevented from crossing vertically by a horizontal dual path.

Finally, $\Pi_{\rm hv}(\lambda)$ is the probability of a horizontal crossing cluster that touches both the top and bottom. Hence,

$$\begin{aligned}\Pi_{\rm hv}(\lambda) &= \Pi_{\rm h}^{b}(\lambda) - \Pi_{\rm h\bar{v}}^{b}(\lambda) = \Pi_{\rm h}^{b}(\lambda) - \Pi_{\rm h}^{\bar{b}}(\lambda)\\ &= \Pi_{\rm h}(\lambda) - \Pi_{\rm h\bar{v}}(\lambda).\end{aligned} \tag{47}$$

Thus, by integrating and combining our new first-crossing densities, we arrive at Watts' equation (2) for the horizontal–vertical crossing probability.

Equations (45) and (46) can also be derived by a duality argument, which is a non-trivial check of our results. To do this, extend our notation, as shown in figure 5. The b and t ($\bar{b}$ and $\bar{t}$) superscripts denote configurations for which there is a horizontal crossing cluster which touches (does not touch) the bottom or top edge of the rectangle, respectively. The four rightmost diagrams in figure 5 include all the configuration types consistent with $\Pi_{\rm h\bar{v}}$.

Thus,

$$\begin{aligned}\Pi_{\rm h\bar{v}} &= \Pi_{\rm h\bar{v}}^{b\bar{t}} + \Pi_{\rm h\bar{v}}^{\bar{b}t} + \Pi_{\rm h\bar{v}}^{bt} + \Pi_{\rm h\bar{v}}^{\bar{b}\bar{t}},\\ \Pi_{\rm h}^{\bar{b}} &= \Pi_{\rm h\bar{v}}^{\bar{b}t} + \Pi_{\rm h\bar{v}}^{\bar{b}\bar{t}},\end{aligned}$$

and

$$\Pi_{\rm h}^{b} = \Pi_{\rm hv} + \Pi_{\rm h\bar{v}}^{b\bar{t}} + \Pi_{\rm h\bar{v}}^{bt}.$$

But by duality $\Pi_{\rm h\bar{v}}^{b\bar{t}} = \Pi_{\rm h\bar{v}}^{\bar{b}t}$ and $\Pi_{\rm h\bar{v}}^{bt} = \Pi_{\rm h\bar{v}}^{\bar{b}\bar{t}}$, from which (45) and (46) follow.

Finally, we derive the expected number of horizontal crossing clusters using $\nu_{\rm h}(\alpha, \beta)$. Recall that this density gives the probability that there is a new cluster spanning from α to β

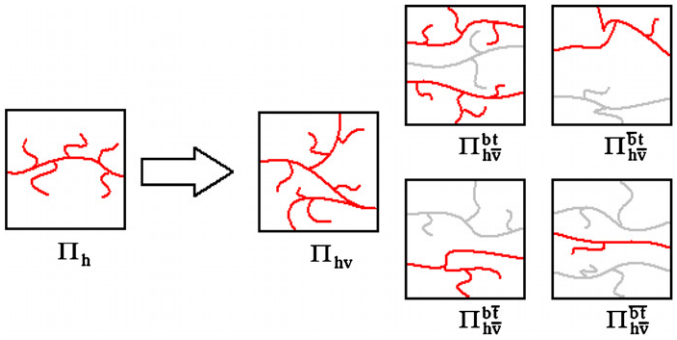

Figure 5. The five distinct configurations that contribute to Π_{h}. Paths in clusters are red, dual paths grey.

that is *not* the lowest crossing cluster in the rectangle. Thus integrating it gives a contribution of $n-1$ for each configuration with n crossing clusters. Therefore,

$$\begin{aligned}\mathcal{N}_{\mathrm{h}}(\lambda)-\Pi_{\mathrm{h}}(\lambda) &= \int_0^{\lambda}\int_1^{\infty} \nu_{\mathrm{h}}(\alpha,\beta)\,\mathrm{d}\beta\,\mathrm{d}\alpha \\ &= \int_0^{\lambda}\int_1^{\infty}\left(\frac{\sqrt{3}}{4\pi(\beta-\alpha)^2}--\pi_{\mathrm{h}}^{\bar{b}}(\alpha,\beta)\right)\mathrm{d}\beta\,\mathrm{d}\alpha \\ &= \frac{\sqrt{3}}{4\pi}\log\left(\frac{1}{1-\lambda}\right)-\frac{1}{2}\Pi_{\mathrm{h\bar{v}}}(\lambda), \end{aligned} \tag{48}$$

giving (4).

This concludes our derivation of the crossing formulae. As mentioned, by exploiting our new crossing results, we obtain all three known results without reference to the q-state Potts model or use of higher-order null vectors. Next, we consider our use of ψ_3 above from an operator point of view and examine some of its consequences.

6. Operator identities

In this section, we first consider our use of the ψ_3 operator in sections 2 and 3, and then present a calculation of the constant K used to normalize our densities (see (8), (9), and section 3).

To begin, consider (8), which, in light of (5) and (7), can be interpreted as replacing $\partial_z\psi_1(z)$ by $K\psi_3(z)$. Now, generally, this would not be possible, since the derivative of a primary operator is not primary itself. However, the derivative of a primary operator of weight zero (like ψ_1) is indeed primary.

Next, (5) gives

$$\begin{aligned}\partial_\alpha\Pi_{\mathrm{h}}(\alpha) &= \partial_\alpha\langle\psi_1(0)\psi_1(\alpha)\psi_1(1)\psi_1(\infty)\rangle \\ &= \langle\psi_1(0)L_{-1}\psi_1(\alpha)\psi_1(1)\psi_1(\infty)\rangle. \end{aligned} \tag{49}$$

Now the weight of $L_{-1}\psi_1$ is 1, the same as for ψ_3. More importantly, the null operator for $\psi_3 := \phi_{1,4}$ is

$$\mathcal{D}_{1,4} = 3L_{-1}^4 - 20L_{-2}L_{-1}^2 + 24L_{-2}^2 + 24L_{-3}L_{-1} - 24L_{-4}. \tag{50}$$

(Here $\mathcal{D}_{r,s}$ denotes the null operator for the $\phi_{r,s}$ Kac operator.) Further, by the L_m commutation relations (for $c = 0$) one has

$$\begin{aligned} &\mathcal{D}_{1,4}L_{-1} = \left(L_{-1}^3 - 6L_{-2}L_{-1} + 6L_{-3}\right)\left(3L_{-1}^2 - 2L_{-2}\right), \text{ i.e.} \\ &\mathcal{D}_{1,4}\mathcal{D}_{1,1} = \mathcal{D}_{3,1}\mathcal{D}_{1,2}. \end{aligned} \tag{51}$$

The right-hand side is exactly the level five null operator used by Watts [9]! Since $\mathcal{D}_{1,2} = 3L_{-1}^2 - 2L_{-2}$ is the null operator for ψ_1, so is $\mathcal{D}_{1,4}\mathcal{D}_{1,1}$ as well.

Therefore, the weight of $L_{-1}\psi_1$ equals that of ψ_3, and they both obey the same null state. Thus correlation functions involving them obey the same differential equations and the solutions must overlap. Hence we posit

$$L_{-1}\psi_1(x) = K\psi_3(x). \tag{52}$$

In section 7, we discuss implications of this equation. For the moment, consider the question as to where in the above it actually makes a difference, i.e., if we were to differentiate a correlation function containing ψ_1 instead of substituting $K\psi_3$ for it, what would change? It is easy to see that the results of section 2 would be the same; however, a crucial difference occurs for (20). Here, the conformal block $\mathcal{F}^4$, which contributes to π_{h}^b, $\pi_{\mathrm{h}}^{\bar{b}}$ and ν_{h}, would not appear, and our calculations would not be valid.

Now we determine the constant K by comparing leading terms in the operator product expansions

$$\begin{aligned} (L_{-1}\psi_1(x))\psi_1(0) &= \partial_x\psi_1(x)\psi_1(0) \\ &= \partial_x\left(\mathbf{1}(0) + \frac{1}{5}x^2T(0) + \cdots + C_{112}x^{1/3}\psi_2(0) + \cdots\right) \\ &= \frac{2}{5}xT(0) + \cdots + \frac{C_{112}}{3}x^{-2/3}\psi_2(0) + \cdots, \end{aligned} \tag{53}$$

and

$$\psi_3(x)\psi_1(0) = C_{123}x^{-2/3}\psi_2(0) + \cdots + C_{134}x\psi_4(0) + \cdots. \tag{54}$$

Thus

$$L_{-1}\psi_1(x) = \frac{C_{112}}{3C_{123}}\psi_3(x) = \frac{3^{1/4}}{2\sqrt{\pi}}\psi_3(x), \tag{55}$$

so that K is indeed given by (9). Note that it appears as a ratio of boundary operator product expansion coefficients, rather than the derivative of the weight $h_1 := h_{(1,2)}$ with the respect to the Potts parameter q, as in [10]. In fact our result for K also implies that

$$h_1'(1) = \frac{1}{2}\left(h_2(1)\frac{C_{112}}{C_{123}}\right)^2, \tag{56}$$

where the evaluations are at $q = 1$.

7. Discussion

In this section, we discuss a few implications of our calculations above, especially the relation (52) (see also (55)).

The full consequences of (52) remain to be explored. However, this relation appears to be supported by representation theory, according to which the highest-weightspaces of a Verma module are one dimensional [19], so that any two primary operators of the same weight must be proportional, as in (52). It is also interesting that the integral weights for the $c = 0$ primary

operators are exactly the Euler pentagonal numbers [20]. There are indications that relations similar to (52) hold for all of them. This suggest the presence of some additional symmetry for conformal field theory with $c = 0$.

Next, consider the seventh-order null vector, which again factorizes in two ways:

$$\mathcal{D}_{3,2}\mathcal{D}_{1,1} = \mathcal{D}_{1,5}\mathcal{D}_{1,2}. \tag{57}$$

Thus, arguing as above, one finds that $L_{-1}\psi_1$ obeys $\mathcal{D}_{3,2}$ as well as $\mathcal{D}_{1,4}$ null vector conditions.

Consider now the fusion rules of an arbitrary Kac table operator with $\phi_{1,4}$ and $\phi_{3,2}$. In general, one has

$$[\phi_{1,4}] \times [\phi_{r,s}] = [\phi_{r,s-3}] + [\phi_{r,s-1}] + [\phi_{r,s+1}] + [\phi_{r,s+3}] \tag{58}$$

$$[\phi_{3,2}] \times [\phi_{r,s}] = [\phi_{r-2,s-1}] + [\phi_{r,s-1}] + [\phi_{r+2,s-1}] + [\phi_{r-2,s+1}] + [\phi_{r,s+1}] + [\phi_{r+2,s+1}]. \tag{59}$$

The above then implies that only families present in both of these should be contained in the $L_{-1}\psi_1$ fusion rule. This leads to

$$[L_{-1}\psi_1] \times [\phi_{r,s}] = [\phi_{r,s-1}] + [\phi_{r,s+1}] = [\psi_1] \times [\phi_{r,s}]. \tag{60}$$

Since ψ_1 and $L_{-1}\psi_1$ belong to the same conformal family, they should transform among the same conformal families under fusions, in agreement with (60).

Thus, our use of ψ_3 to obtain the crossing densities augments the $[\psi_1]$ conformal family. The two additional families present in (58) generate crossing configurations that are more complicated than those that can be generated by ψ_1 operators alone. Specifically, the inclusion of the ψ_3 operator allowed us to make use of the $[\psi_3] \times [\phi_{r,s}] = [\phi_{r,s+3}]$ fusion which gives configurations of the type shown in figure 2(*C*).

We can also use the actions of the fifth and seventh level null vectors on the identity operator to deduce properties of the stress tensor T. Now

$$\begin{aligned}\mathcal{D}_{1,2}\mathbf{1}(z) &= \left(3L_{-1}^2 - 2L_{-2}\right)\mathbf{1}(z) \\ &= -2T(z).\end{aligned} \tag{61}$$

Using (51) and (57) then shows that the stress tensor is annihilated by both $\mathcal{D}_{3,1}$ and $\mathcal{D}_{1,5}$. (Note that when $c = 0$, T is a primary operator.)

Further, as argued for $\psi_3 \propto L_{-1}\psi_1$, only the conformal families contained in both $\phi_{3,1}$ and $\phi_{1,5}$ fusions should appear in fusions with the stress tensor, which yields

$$[T] \times [\phi_{r,s}] = [\phi_{r,s}]. \tag{62}$$

This is as expected, since the stress tensor generates conformal transformations of conformal families amongst themselves.

We hope to explore, elsewhere, the consequences of these remarks, including the 'overlap' of T and $\psi_4 := \phi_{1,5}$ in analogy with the result for $L_{-1}\psi_1$ and ψ_3.

Acknowledgments

This work was supported in part by the National Science Foundation Grants Nos DMR-0203589, DMR-0536927 (PK) and DMS-0553487 (RMZ).

References

[1] Cardy J L 1992 Critical percolation in finite geometries *J. Phys. A: Math. Gen.* **25** L201–6 (*Preprint* hep-th/9111026)

[2] Kleban P, Simmons J J H and Ziff R M 2006 Anchored critical percolation clusters and 2D electrostatics *Phys. Rev. Lett.* **97** 115702 (*Preprint* cond-mat/0605120)
[3] Kleban P and Zagier D 2003 Crossing probabilities and modular forms *J. Stat. Phys.* **113** 431–54 (*Preprint* math-ph/0209023)
[4] Duplantier B 2003 Higher conformal multifractality *J. Stat. Phys.* **110** 691–738 (*Preprint* cond-mat/0207743)
Duplantier B 2003 Conformal fractal geometry and boundary quantum gravity *Preprint* math-ph/0303034
[5] Dubédat J 2006 Excursion decompositions for SLE and Watts' crossing formula *Probab. Theory Relat. Fields* **134** 453–88 (*Preprint* math.PR/0405074)
[6] Aizenman M 1998 *Scaling Limit for the Incipient Spanning Clusters (Mathematics of Multiscale Materials; The IMA Volumes in Mathematics and its Applications)* ed K Golden, G Grimmett, R James, G Milton and P Sen (Berlin: Springer) (*Preprint* cond-mat/9611040)
[7] Smirnov S 2001 Critical percolation in the plane *C. R. Acad. Sci. Paris Sér. I Math.* **333** 239–44
[8] Simmons J J H and Kleban P (in preparation)
[9] Watts G 1996 A crossing probability for critical percolation in two dimensions *J. Phys. A: Math. Gen.* **29** L363–8 (*Preprint* cond-mat/9603167)
[10] Cardy J 2001 Conformal invariance and percolation *Preprint* mathph/0103018
[11] Cardy J 2000 Linking numbers for self-avoiding loops and percolation: application to the spin quantum Hall transition *Phys. Rev. Lett.* **84** 3507–10 (*Preprint* cond-mat/9911457)
[12] Smirnov S unpublished
[13] Maier R S 2003 On crossing event formulas in critical two-dimensional percolation *J. Stat. Phys.* **111** 1027–48 (*Preprint* math-ph/0210013)
[14] Lewellen D C 1992 Sewing constraints for conformal field theories on surfaces with boundaries *Nucl. Phys.* B **372** 654–82
[15] Abramowitz M and Stegun I A (ed) 1968 *Handbook of Mathematical Functions (National Bureau of Standards Applied Mathematics Series)*
[16] Ziff R M, Cummings P T and Stell G 1984 Generation of percolation cluster perimeters by a random walk *J. Phys. A: Math. Gen.* **17** 3009–17
[17] Grassberger P 1986 On the hull of two-dimensional percolation cluster perimeters *J. Phys. A: Math. Gen.* **19** 2675–7
[18] Simmons J J H, Kleban P, Dahlberg K and Ziff R M 2007 The density of critical percolation clusters touching the boundaries of strips and squares *J. Stat. Mech.* P06012
[19] Rocha A 2006 Private communication
[20] Rocha-Caridi A and Wallach N R 1983 Characters of irreducible representations of the Lie algebra of vector fields on the circle *Invent. Math.* **72** 57–75